**Title**
Finite Element Modeling of Burr Formation in Metal Cutting



**Authors**
Min, Sangkee
Dornfeld, David
Kim, J.
et al.

**Publication Date**
2007-06-27

# FINITE ELEMENT MODELING OF BURR FORMATION IN METAL CUTTING

S. Min[1], D. A. Dornfeld[1](1), J. Kim[1], B. Shyu[1]
[1]Laboratory for Manufacturing Automation, Dept. of Mechanical Engineering
University of California, Berkeley, CA, U.S.A.

**Abstract**
In order to advance understanding of the burr formation process, a series of finite element models are introduced. First a finite element model of the burr formation of two-dimensional orthogonal cutting is introduced and validated with experimental observations. A detailed and thorough examination of the drilling burr forming process is undertaken. This information is then used in the construction of an analytical model and, leads to development of a three-dimensional finite element model of drilling burr formation. Using the model as a template, related burr formation problems that have not been physically examined can be simulated and the results used to control process planning resulting in the reduction of burr formation. We highlight this process by discussing current areas of research at the University of California in collaboration with the Consortium on Deburring and Edge Finishing (CODEF).

Keywords: Burr, Finite element method (FEM), Modeling

## 1 INTRODUCTION

Since the middle of the 18$^{th}$ century when metal started to be used in engineering structures, metal cutting has evolved into one of the most adaptable metal working processes [1]. Its use exploded as the Industrial Revolution promoted mass production and its techniques expanded into sub categories such as milling, turning, drilling and so forth. However, development and usage of metal cutting techniques lacked a basic understanding of the fundamental mechanism and caused stagnation in enhancement of the process. One of the first acknowledged attempts of modelling metal cutting was by Ernst and Merchant [2] around World War II. This was slowly followed by many successors.

In the past, most modeling efforts remain with 2-D orthogonal cutting and describe only steady-state cutting. The importance of the final stage of cutting, tool exit, which creates burrs and other edge defects has been largely ignored. It should be understood because the burr damages the final precision integrity of parts and requires an additional process, deburring, which can cause dimensional inaccuracy, change surface integrity of machined workpiece, and sometimes result in irrecoverable damage on the parts [3]. In the middle of 1970's, the first quantitative analysis of burr formation in 2-D orthogonal cutting based on experimental observation was performed by Gillespie and Blotter [4]. They characterized the burr formation as a result of bending deformation which occurred at the end of the workpiece. Many experimental approaches to model burr formation have followed in the last two decades.

However, experimental approaches have always been limited by specific tool geometries, workpiece materials and cutting conditions. They were not able to deal with the tremendous number of parameters involved in cutting processes. Several analytical approaches were attempted but were still based on experimental observation mixing plastic theory and geometrical description of burr formation [5]. It is very difficult to derive a closed form analytical solution for burr formation because it involves complicated thermal-elastic-plastic behavior of workpiece material under large deformation with high strain rate. The lack of precise material models describing material behavior under high strain rate blocked further pursuit of analytical modeling of burr formation with plastic theory and pushed it in the direction of geometrical conformation theory with energy balance [6].

The tremendous development of computing technology in the last two decades makes the finite element method very attractive in the modeling of burr formation. Many modeling efforts using FEM evolved with increasing computing power and a number of decent models of 2-D orthogonal cutting in steady-state were proposed [7]. However, modeling of burr formation is very different from that of steady-state cutting because values used to model chip formation change as the tool approaches the exit surface of workpiece. Hence, a very limited number of FE models of burr formation in 2-D orthogonal cutting and drilling have been proposed. As new models of material behavior under high strain rate appear [8], many aspects of FE models of metal cutting including burr formation will be tuned more realistically. In this study, the FE modeling of burr formation from 2-D orthogonal cutting to 3-D drilling is reviewed.

## 2 FINTE EELEMENT MODEL OF BURR FORMATION IN 2-D ORTHOGONAL CUTTING

### 2.1 Failure criterion

The essence of metal cutting in reality is removal of material from workpiece regardless of the machining process. How to model this concept is the biggest challenge in finite element modeling of metal cutting. In most cases, this concept is simulated either by separation of elements or by removal of elements in the model. Due to the complexity of the problems, FE modeling research started with two-dimensional orthogonal cutting focusing only on steady-state cutting. As modeling techniques advanced and experimental information accumulated, a thorough model from steady-state cutting to the final burr formation in two-dimensions was developed.

The chip separation criteria are related to the separation of elements that are mostly adopted in 2-D orthogonal cutting. Hence, it is a more commonly used term in 2-D orthogonal cutting than failure criterion. Even though different measures for the chip separation criteria were used, the criteria were applied in the same way in a range of work [9-11]. The parting line between the workpiece and the chip was predefined and the chip was formed when the element near the parting line met the separation criterion.

### 2.2 Burr formation stages

Park and Dornfeld developed the finite element model of the burr formation in 2-D orthogonal cutting with a plane strain assumption and investigated the influences of various process parameters [12,13]. A general purpose FEM software package, ABAQUS, was used to simulate the chip and burr formation processes, especially transition from steady-state cutting to burr formation. An adiabatic heating model was adopted to simulate the heat generation effects due to plastic work of the workpiece and chip. Also, based on a ductile failure model offered by ABAQUS, the metal cutting simulation procedure was developed to separate the chip from the workpiece and to give a final burr/breakout configuration. The burr formation mechanism is divided into four stages: initiation, initial development, pivoting point, and final development. The results from the FEA are qualitatively verified with experimental data, Figure 1.

The initiation stage represents the point where the plastically deformed region appears on the edge of the workpiece. In the initial development stage, significant deflection of the workpiece edge occurs, and a bending mechanism initiates burr formation. In the pivoting point stage, material instability occurs at the edge of the workpiece. In the final development stage, a burr is further developed with the influence of the negative deformation zone formed by a shearing process. Hence, plastic bending and shearing are the dominant mechanisms in this stage. However, if the material cannot sustain highly localized strain in front of the tool edge, then fracture is initiated and leads to the edge breakout phenomenon.

### 2.3 Burr minimization using a backup material

Park inherited the idea of minimizing burr formation using a backup material from Gillespie [14] who conducted experiments to examine the backup material influence for burr minimization in drilling. In order to effectively minimize the burr size, three cases of back-up material influence on burr formation processes were examined.

With the thick backup material, Figure 2 (a), continuous chip formation continues until the tool exits the cut at the very end of the workpiece, and fracture takes place at the last moment. Consequently, the burr can be effectively minimized. With the thin backup material, Figure 2 (b), the whole backup material exhibits bending characteristics. The bending of the backup material results in a large gap between the two materials. In this case, the burr size can also be effectively minimized although a relatively large remnant, compared to the thick backup material case, would be expected to be left at the edge. As a result, it would be desirable to have backup materials thick enough to cause only local deformation near the edge of the workpiece by avoiding the bending of the backup material.

Figure 2 (c) shows the case when the thin backup material contacts the workpiece up to the pre-defined machined surface. A similar case has been experimentally carried out by Gillespie to minimize the size of a drilling burr. Although orthogonal cutting is quite different from drilling, the characteristics of the roll-over process in orthogonal cutting are similar to those seen in drilling. Initially, the deflection of the edge above the pre-defined machined surface takes place instead of forming a gap between the two materials. As a result, this effectively reduces the size in any resulting burr and would be also the mechanism behind minimizing the size of a drilling burr in Gillespie's experiment. Hence, the burr size could be effectively minimized when the back-up material supports the workpiece only up to the pre-defined machined surface.

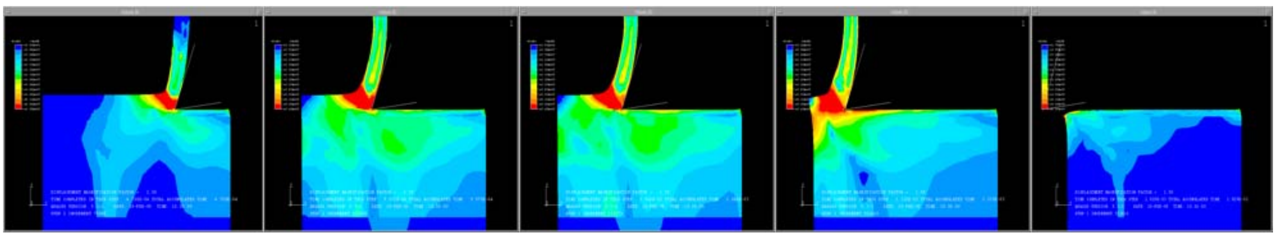

(a) Steady-state (b) Initiation (c) Development (d) Pivoting (e) Burr

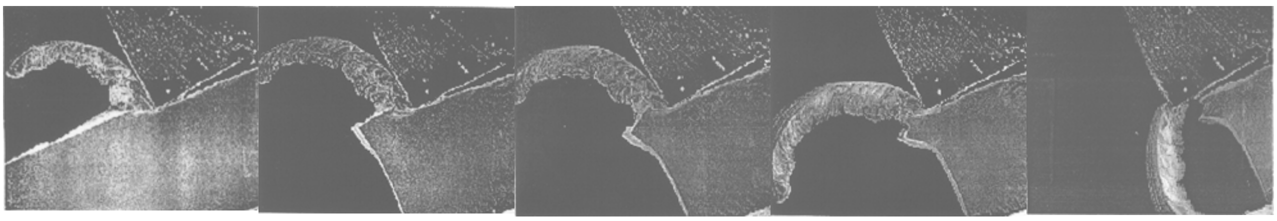

(f) Steady-state (g) Initiation (h) Development (i) Pivoting (j) Burr

Figure 1: Comparison between finite element simulation (top) and SEM (bottom) pictures of burr formation mechanism in 2-D orthogonal cutting [12].

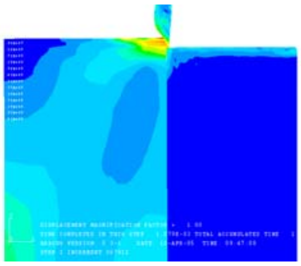

(a)

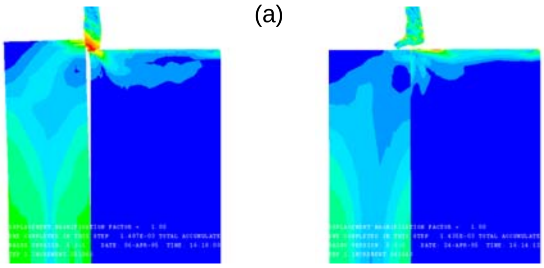

(b) (c)

Figure 2: Equivalent stress contour with backup materials, (a) thick backup, (b) thin backup, (c) thick backup partially supporting workpiece [13].

## 3 ANALYTICAL MODELING OF DRILLING BURR FORMATION

### 3.1 Burr types

One of the most widely used processes in metal cutting is the drilling process. Hence, extensive experimental studies of the drilling burr problem have been made [15]. The drilling burr has various shapes and size depending on the influencing parameters.

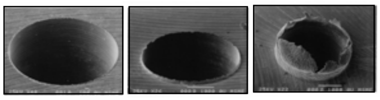

(a) Low alloy steel (AISI 4118)

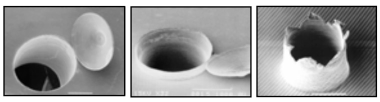

(b) Stainless steel (AISI 304L)

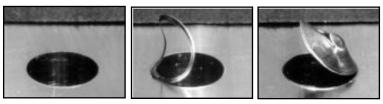

(c) Titanium alloy (Ti-6Al-4V)

(d) Aluminum alloy (6061)

Figure 3: Various types of drilling burrs

Figure 3 shows some examples of drilling burrs observed in drilling several materials. The left-hand pictures of each row represent burrs produced in relatively low feed and cutting speed, while right-hand pictures are for high feed and speed. When the feed and the cutting speed are low, the drilling burr tends to have a uniform shape along the hole periphery for most materials. The workpiece property makes a big difference when the feed and the cutting speed increase. When the material has moderate ductility, the material tends to elongate to some extent during burr formation, resulting in a large burr height and burr volume, Figure 3 (a), (b) and (c). However, if the material is quite brittle, catastrophic fracture occurs as the feed and the speed increases, resulting in irregular burrs having several large chunks, lobes, or petals as shown in Figure 3 (d).

Observing the kinematics of drilling burr formation gives us more insight into the burr formation mechanism. Even though the final burr shapes can look alike, the burr formation mechanim can be substantially different. Figure 4 shows proposed burr formation mechanisms for several burr shapes, matched with coresponding pictures observed by a high-speed video while drilling low alloy steel, AISI 1018, from [16].

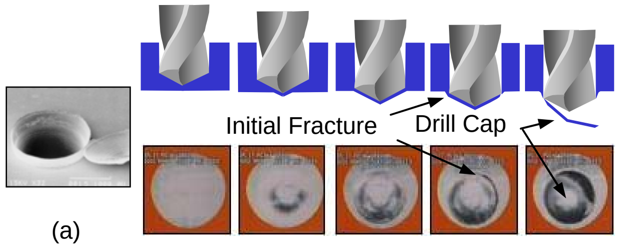


(a)

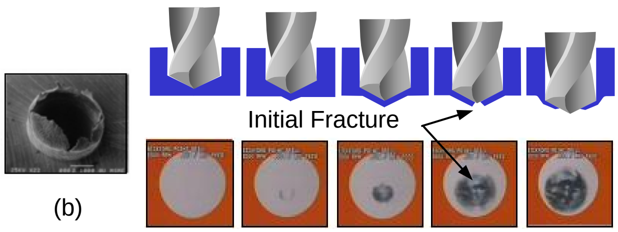


(b)

Figure 4 : Proposed burr formation mechanisms, (a) uniform burr, (b) crown burr [17].

### 3.2 Analytical model

An analytical model for drilling burr formation was developed by Kim based on the observation of the behavior of workpiece material during drilling of low alloy steel and the principle of energy conservation and metal cutting theory [17]. The model holds for ductile materials that do not show catastrophic fracture during the plastic deformation of workpiece material for burr formation. The thrust force is expressed as

$$F_{th} = \frac{\sqrt{2}}{3} R f \left(\frac{\sigma_u}{\sigma_y}\right) \sigma_y \cdot \sum_{i=1}^{N} \left\{ \frac{\sin\left(\frac{\pi}{6} - \frac{\alpha_d}{2}\right)\left(\rho_{i+1} - \rho_i\right)}{\sin\left(\frac{\pi}{6} + \frac{\alpha_d}{4}\right)\cos\left(\frac{\pi}{3} - \frac{\alpha_d}{4}\right)} \right\} \qquad (1)$$

where $R$ is a drill radius, $f$ feed, $\sigma_y$ tensile yield strength, $\sigma_u$ ultimate strength, $N$ is the number of segments along a cutting edge of the drill, $\alpha_d$ dynamic rake angle, $\rho_i$ relative radius of $i$th segment.

Burr height and thickness can be calculated by equation (2).

$$H = t_0 \sin p \exp\left\{ \frac{\sqrt{3}}{2} \ln\left( \frac{100}{100 - \%R.A.} \right) \right\} \qquad (2)$$

$$T = t_0 \sin p \tan p$$

where $H$ , $T$ are burr height and thickness respectively, and $2p$ is point angle, $\%R.A.$ is percent reduction in area of material at ensile fracture, $t_o$ is the initial thickness of deforming material beneath the drill and given by equation (3).

$$t_0 = \frac{1}{2X}\left( -Y + \sqrt{Y^2 - 4XZ} \right)$$

$$X = \frac{3}{4}\pi \sin^3 p \cos p + \frac{1}{2}\pi\left(\frac{\pi}{2} - p\right)$$

$$Y = \frac{3}{4}\pi R \sin p \ln\left(\frac{1}{\sin p}\right) - \frac{2}{9}\frac{f}{\tan p} R \left(\frac{\sigma_u}{\sigma_y}\right) \cdot \Phi$$

(3)

### 3.3 Results

Experimental validation of Kim's model with stainless steel (AISI304L) is shown in Figure 5. Split point twist drills were used for the experiments. The model can be effectively used to investigate the effects of other influencing parameters, as shown in Figure 6. It shows burr height and thickness variation within a range of one parameter while holding the other parameters at the values shown in Table 1.

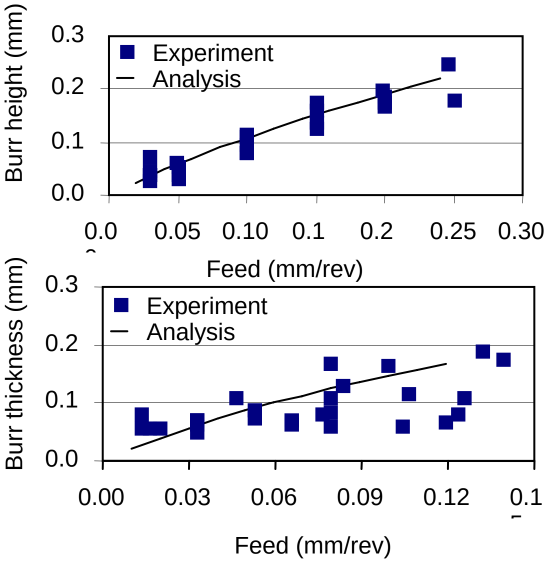


Figure 5: Comparison of burr height and thickness between experiments and analysis in AISI 304L(d=1.984 mm).

| | | | |
|---|---|---|---|
| Drill diameter (mm) | 3.968 | Feed rate (mm/rev) | 0.08 |
| Point angle (deg) | 135 | Web thickness ratio | 0.38 |
| Helix angle (deg) | 25 | $\sigma_u$ / $\sigma_y$ | 2.2 |

Table 1: Parameters used for analytical investigation

## 4 FINITE ELEMENT MODELING OF DRILLING BURR FORMATION

The analytical model is, however, for very limited conditions. Combining the modeling techniques of 2-D and observations from experiments and the analytical model, a 3-D finite element model of the drilling burr formation was developed.

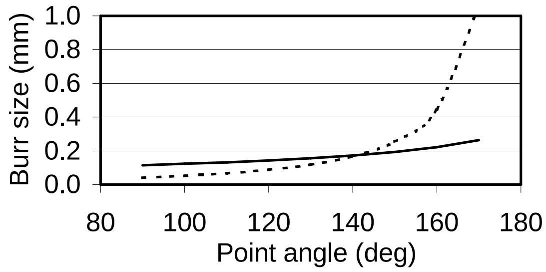


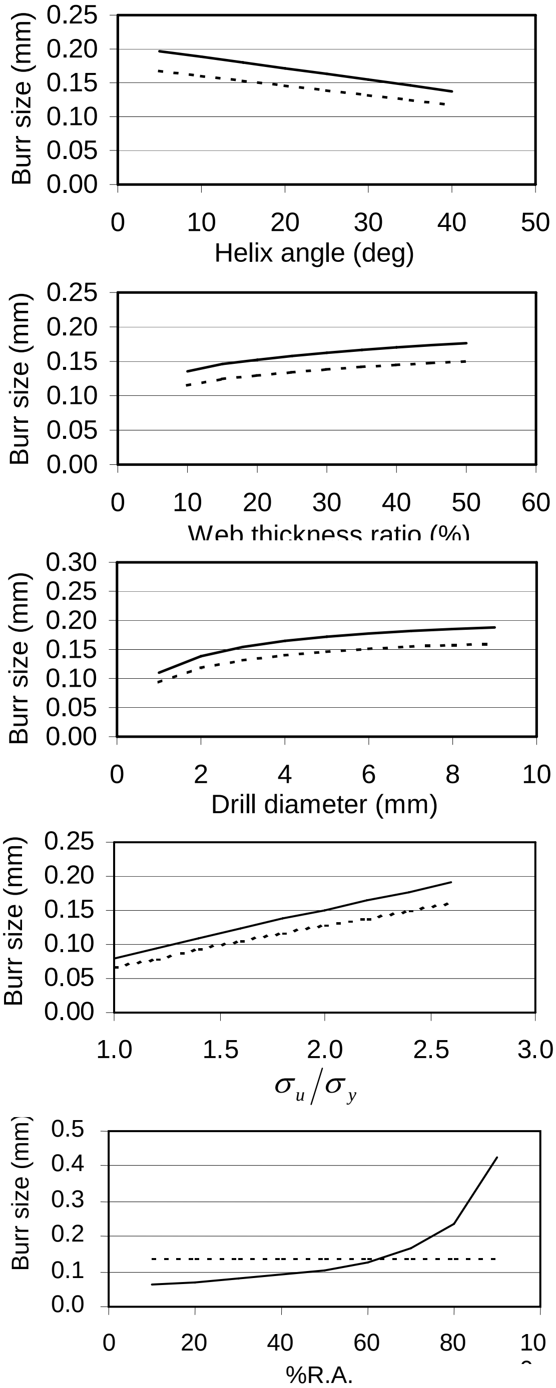


Figure 6: Effects of various parameters on drilling burr size(Solid line: burr height, dashed line: burr thickness)

### 4.1 Failure criterion

Unlike the modeling of 2-D orthogonal cutting, it is much more difficult to define a parting line and arrange elements along this parting line in driling because the material in front of drill deforms as the drill advances and at any instance, this causes the parting line to be redefined. Instead, elements closed to the drill tip were removed when all the material points in an element meet a failure criterion.

Material failure was assumed to occur when the damage parameter, $\omega$, the ratio of the incremental equivalent plastic strain to the equivalent plastic strain at failure exceeds one. Once an element satisfies the failure criterion, it then becomes inactive in the remaining calculations [18].

$$\omega = \sum \left( \frac{\Delta \bar{\varepsilon}^{pl}}{\bar{\varepsilon}_f^{pl}} \right) \geq 1 \qquad (4)$$

### 4.2 Drill modeling

Although the results of a FE model can be useful, they were not being used in a manner that could have maximum potential impact on the drilling process due to the high cost of preparation for the process simulation. With a strong demand in industry for burrless hole making, it is desired to integrate FEA models with drill CAD to evaluate drill performance in the drilling process and fully utilize the benefits of this numerical tool in concurrent engineering. Modeling the complexity and various geometry parameters of a drill is consuming work. Hence, a mathematical model of a twist drill was proposed by Tsai and Wu [19] and an integrated CAD/FEA system for drill design and drilling burr formation simulation was proposed by Guo and Dornfeld [20].

The enhanced CAD/FEA software was developed as shown in Figure 7. The drill bit design software lets users select drill geometric parameters, such as point angle and twist angle, to define drill geometry. A graphical view of the drill bit gives users real time feedback on the drill geometry determined by the current values of drill geometric parameters. After the geometry is determined, an FE mesh of the drill is generated.

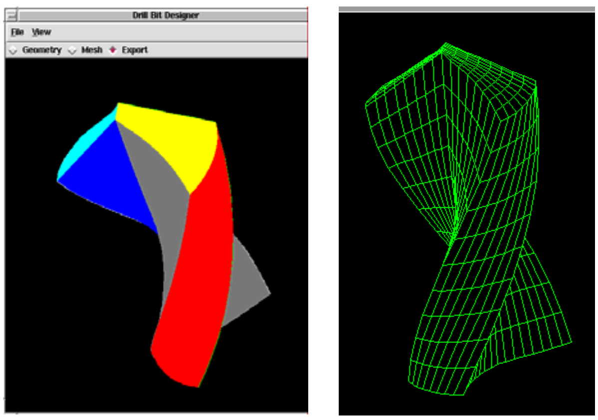


(a) solid model (b) FEM mesh

Figure 7: Drill bit design software

### 4.3 FE modeling assumptions

Incremental plasticity using von Mises yield surface and associated flow rule were used to model the plastic behavior of the material. All the material properties were assumed to be isotropic. The strain rate dependency of material properties was modeled using the overstress power law because material properties, especially yield stress, vary at high strain rate (strain rate in drilling ranges from $10^3$ to $10^5$). Heat is generated mostly by inelastic strain. Since a drilling process is an enclosed process which involves high strain rate, heat cannot be dissipated through the workpiece. Hence, an adiabatic thermal assumption was made. Built-up-edge and chip formation were not considered due to the complexity of the problem. Process parameters from experiments that generate a uniform burr and a crown burr were chosen.

| | | | |
|---|---|---|---|
| | Proposed burr formation mechanism [15] | FEM simulation | High-speed camera image [16] |

### 4.4 Burr types and formation mechanisms

Depending on the cutting conditions, two different types of burrs, a uniform burr and a crown burr, were simulated for stainless steel (AISI 304L). Uniform burrs were created in general at low speed and low feed and crown burrs at high feed and high speed. The burr formation mechanism is divided into five stages: (a)steady-state, (b)initiation, (c)development, (d)initial fracture, and (e)final burr formation for both burr types in Table 2 and Table 3. The thrust force induced by many cutting parameters causes different initiation points and initial fracture locations, which lead to different burr types.

During the steady-state cutting stage, material in front of the drill tip is removed as elements comprising that portion meet the failure criterion and a plastic zone appears at the center of the drill tip. As the drill advances, the plastic zone at the center of the drill tip reaches the exit surface of the workpiece at the burr initiation stage. In a uniform burr, this plastic zone appears at the exit surface of the workpiece when the drill almost reaches the exit surface. Hence, the layer between the exit surface and the drill tip is thin. By contrast, the plastic zone reaches the exit surface when the drill is far away from that surface and forms a thick plastic layer in a crown burr, Figure 8.

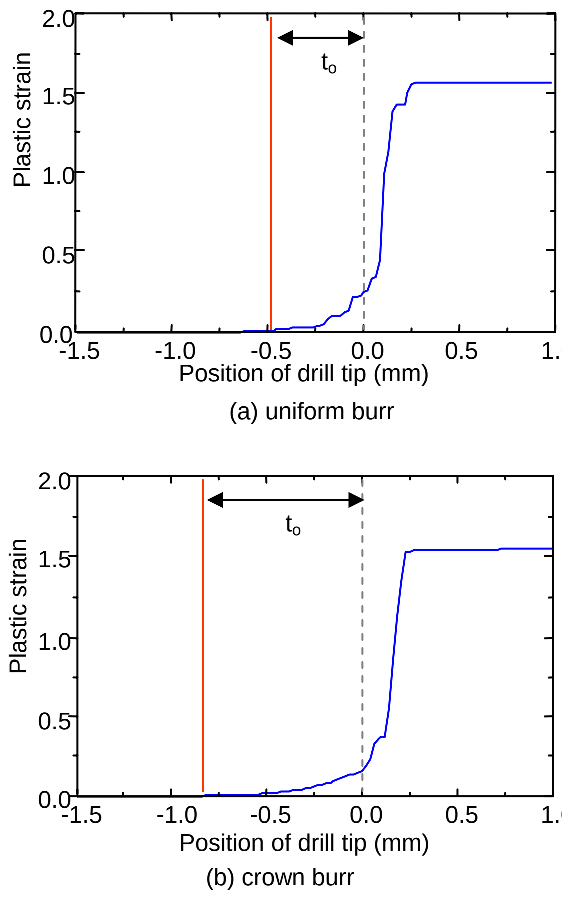


(a) uniform burr

(b) crown burr

initiation point exit surfaceInitiation

$t_o$ initiation thickness

Figure 8: Comparison of the burr initiation point of a uniform burr and a crown burr by FEM

| | | | |
|---|---|---|---|
| a | 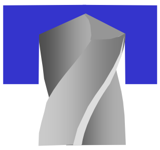 | 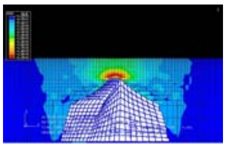 |  |
| b | 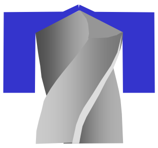 | 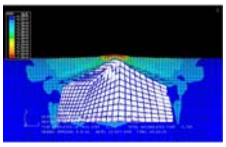 |  |
| c | 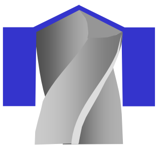 | 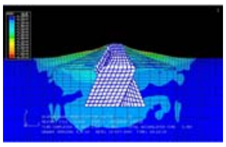 |  |
| d | 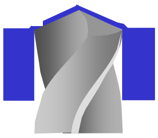 | 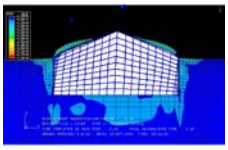 |  |
| e | 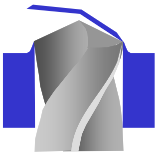 |  |  |

Table 2: Burr formation mechanism of a uniform burr

| | Proposed burr formation mechanism [15] | FEM simulation | High-speed camera image [16] |
|---|---|---|---|
| a | 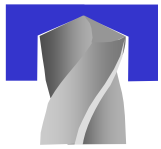 | 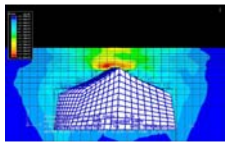 |  |
| b | 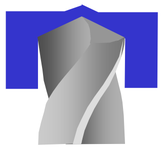 | 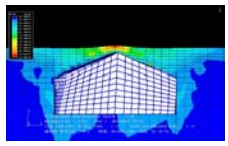 |  |
| c |  | 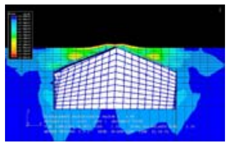 |  |
| d | 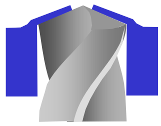 | 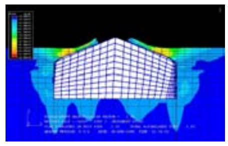 |  |
| e | 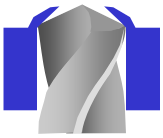 | 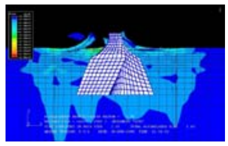 |  |

Table 3: Burr formation mechanism of a crown burr

The thickness of the layer at the burr initiation point defines the burr formation behavior in the following stages: development and initial fracture. The thin layer of the plastic zone in the uniform burr does not have enough support to be cut by the drill and so very little cutting at the perimeter of the drill occurs during the development stage, Table 2 (c). The plastic zone that initially formed near the center of the drill area expands to the edge of the drill. However, the thick layer of the plastic zone in the crown burr enables material to be cut during the development and allows very little expanding of the plastic zone to the edge of the drill, Table 3 (c).

In the uniform burr, the initial fracture occurs at the edge of the drill, Table 2 (d) and it leads the formation of cap, Table 2 (e). In the crown burr, the initial fracture occurs at the center of the drill, Table 3 (d) and the rest of material deforms plastically and forms a crown burr, Table 3 (e).

The five stages of the uniform burr and the crown burr are compared with the proposed mechanism [15] and high-speed camera images (top view) [16] in Table 2 and Table 3. The burr formation mechanism from FE simulation shows good agreement with images from high-speed camera and proposed burr formation mechanism.

## 5 SUMMARY

This paper summarized the research efforts to model burr formation in metal cutting. For simplicity, the finite element model of burr formation in 2-D orthogonal cutting was proposed with experimental validation. This model was able to simulate burr formation for both ductile and brittle materials and gave insightful information on the burr formation mechanism.

Based on observation of drilling burr formation and physical principles, an analytical model was developed to predict drilling burr formation. The model is for ductile materials that produce a uniform burr with a drill cap. This model was successfully developed to predict the final drilling burr size. The model contains the effect of material property, drill geometry and process condition. It also contains several assumptions and simplifications. Burr sizes calculated by the model showed good agreement with experimental results. Effects of other parameters on drilling burr formation were investigated with the model developed. The parameter effects are consistent with burr formation mechanism and the effects of thrust force in drilling.

With accumulated experimental data of drilling burr formation and information provided from 2-D orthogonal cutting and the analytical model of drilling burr formation, a finite element model of 3-D drilling burr formation was proposed. It simulated two different types of burr, a uniform burr and a crown burr, which can be easily found in drilling of ductile materials such as stainless steel and low alloy steel. Burr formation mechanisms for both types of burrs modeled by FEM were validated with experiments. This model can be used to evaluate effects of other parameters on drilling burr formation including part design.

Modeling of burr formation in metal cutting still requires a lot of support from material modeling, tool modeling, and process modeling. Hence, new theories for material behavior, refined software of tool design, and improvement of finite element method with increasing computing power are absolutely necessary for better finite element model of burr formation in metal cutting in the future.

## 6 ACKNOWLEDGMENTS

The authors wish to thank the members of the Consortium on Deburring and Edge Finishing (CODEF) for their discussions, feedback and financial support of this work. Further information can be found at http://lma.berkeley.edu/codef.

## 7 REFERENCES

[1] Trent, E.M., Wright, P.K., 2000, Metal Cutting, Butterworth-Heinemann, Woburn, MA.

[2] Merchant, M.E., 1945, Mechanis of the Metal Cutting Process 1: Orthogonal Cutting and a Type-2 Chip, Journal of Applied Physics, 16/5:267-275.

[3] Gillespie, L.K., 1975, Hand Deburring of Precision Parts, Bendix Corporation Unclassified Topical Report, BDX-613-1443.

[4] Gillespie, L.K., Blotter, P.T., 1976, The Formation and Properties of Machining Burrs, Trans. ASME, J. Engineering for Industry, 98/1:66-74.

[5] Sofronas, A., 1975, The Formation and Control of Drilling Burrs, Ph.D. dissertation, University of Detroit.

[6] Ko, S.L., Dornfeld, D.A., 1991, A Study on Burr Formation Mechanisms, Trans. AMSE, J. Engineering Materials and Technology, 113/1:75-87.

[7] Chen, Z.G., Black, J.T., 1994**,** FEM modeling in metal cutting, Manufacturing Review, 7/2:120-133.

[8] Kopac J. Korosec M., Kuzman K., 2001, Determination of Flow Stress Properties of Machinable materials with Help of Simple Compression and Orthogonal Machining Test, Int. J. Machine Tools and Manufacture, 41:1275-1282.

[9] Iwata K., Osakada K., Terasaka Y., 1984, Process Modeling of Orthogonal Cutting by the Rigid-Plastic Finite Element Method, ASME Trans., J. of Engineering Materials and Technology, 106:132-138.

[10] Komvopoulos K., Erpenbeck S.A., 1991, Finite Element Modeling of Orthogonal Metal Cutting, J. of Engineering for Industry, 113:253-267.

[11] Carroll J.T., Strenkowski J.S., 1988, Finite Element Models of Orthogonal Cutting with Application to Single Point Diamond Turning, Int. J. Mech. Sci., 30:899-920.

[12] Park, I.W., Dornfeld, D.A., 2000, A Study on Burr Formation Processes using the Finite Element Method- Part I, Trans. ASME, J. Engineering Materials and Technology, 122:221-228.

[13] Park, I.W., Dornfeld. D.A., 2000, A Study of Burr Formation Processes using the Finite Element Method- Part II- The Influence of Exit Angle, Rake Angle and Backup Material on Burr Formation Processes, Trans. ASME, J. Engineering Materials and Technology, 122:229-237.

[14] Gillespie, L.K., 1975, Burrs Produced by Drilling, Bendix Corporation Unclassified Topical Report, BDX-613-1248.

[15] Kim, J., Min, S., Dornfeld, D.A., 2001, Optimization and Control of Drilling burr Formation of AISI 304L and AISI 4118 based on Drilling Burr Control Charts, Int. J. Machine Tools and Manufacture, 41/17:923-936.

[16] Furness, R., 1998, High Speed Video of Drilling Burr Formation, AMTD, Ford Motor Company.

[17] Kim, J., 2001, Optimization and Control of Drilling Burr Formation in Metals, Ph.D. Dissertation, University of California, Berkeley.

[18] ABAQUS/Explicit User's Manual, 1998, Hibbit, Karlsson, & Sorenson, Inc., Pawtucket, RI.

[19] Tsai, W.D., Wu, S.M., 1979, A Mathematical Model for Drill Point Design and Grinding, ASME Trans., J. Engineering for Industry, 101:333-340.

[20] Guo, Y., Dornfeld, D.A., 1998, Integration of CAD of Drill with FEA of Drilling Burr Formation, Trans. Of NAMRI/SME, 26:201-206.